

Playing Robot Soccer Outdoor

Matthias Hofmann, Arne Moos, Fabian Rensen, Ingmar Schwarz, and Oliver Urbann²

Abstract—RoboCup is one of the most important benchmarks for humanoid robotics. There has been impressive progress during the last decades. The Standard Platform League (SPL) fosters robotic research on a low-power robotic platform. One of the next major challenges in the upcoming years is to move the competition from classical indoor setups to outdoor or outdoor-like environments. This includes new challenges for the vision system as it has to deal with natural at daytime, or artificial lighting at nighttime. Moreover, artificial lawn will be used in the SPL in upcoming years to improve motion skills of the robots. This paper describes how we handle the new setup that has been introduced with the outdoor competition in 2016 at RoboCup Leipzig.

I. INTRODUCTION AND RELATED WORK

RoboCup is an international initiative that fosters research in robotics and artificial intelligence competitively. The big vision of the RoboCup society is to beat the current world champion of human soccer in 2050 under realistic conditions. Hence, special focus lies on multi-robot systems that collaborate and share a common goal. Particular RoboCup disciplines are Robot Soccer, Robot Rescue, RoboCup@Home, RoboCup Industrial, and RoboCupJunior. RoboCup includes various soccer leagues that focus on different research challenges. In the RoboCup Standard Platform League all teams compete with identical robots. This means that the best software will decide about the championship. The robots operate completely autonomously, and the current standard platform is the NAO robot by SoftBank Robotics.

In order to meet the overall goal of RoboCup, the rules in the Standard Platform Competition are being carefully revised by the Technical Committee of the league every year. This ensures continuous progress in the league since the rule changes impact either the soccer rules themselves, or the environment of the game. Since Past revisions of the rule book have focused on changes affecting mainly the team play between the robots, the vision, and the localization systems of the robot. To this end, the number of robots was increased from three to five robots per team, the field size has significantly grown from four times six meters to six times nine meters. The field goals have become an identical color, first yellow, and in 2015 white. Finally, the ball has changed from an orange hockey ball to a small soft ball with a black and white pattern.

For upcoming years, the SPL will take a next major step, i.e. playing in outdoor-like environment on artificial turf. A first competition has been held at RoboCup 2016 in Leipzig, Germany. Games were held in an Atrium with natural light,

¹Robotics Research Institute, TU Dortmund University, Germany
<forname.surname>@tu-dortmund.de

and on an artificial lawn with a floor height of 15 mm. This paper describes our approach to tackle these major challenges imposed with this setup. The performance of our methodologies are being assessed by analyzing the outdoor competition's final game.

The paper is structured as follows: Section II guides though the major techniques being used for ball detection and the handling of changing lighting conditions. The motion with special focus on sensor control of the body of the robot is presented in Section III. An evaluation of the performance of applied methodologies are presented in Section IV where we analyzed the final game of the outdoor competition of the year 2016 based on log data.

II. VISION

This section describes the current state of our vision system as it was used in RoboCup 2016. The system has been presented in [1] and has been improved and altered for the detection of the current ball [2].

A. Handling Varying Lighting Conditions

The outdoor competition at RoboCup 2016 presented different and new challenges for the competing teams (see Figure 1). Since the fields were inside a glass hall they had to cope with different scenarios within one game. These scenarios include

- looking into sunlight,
- shadows from the ceiling steel beams, spectators and robots or
- fast changes in illumination due to head movement or clouds.

These issues are handled by looking for local edges and gradients instead of relying on absolute predefined values while scanning the image. Furthermore, every object detection algorithm (line, robot and ball) has been altered to rely less on field color detection and more on shape verification.

Since the presentation of our vision system at RoboCup 2015, a more efficient implementation reduced the runtime without the ball detection from 18 ms to less than 10 ms. This enabled us to use a more sophisticated ball detection as described below. Since the goal detection was less reliable than the line detection and did not improve the localization task, it was removed to allow even more runtime for the ball detection.

B. Black-White Ball Detection

In the previous years our vision system did use less than 0.5 ms of runtime on the NAO robot for ball detection since the orange color was unique on the soccer field and very



Fig. 1: Picture of the venue at RoboCup Leipzig 2016.

few image regions had to be scanned. Since the colors on the current ball are present in many parts of the image, possible ball spots generated from our vision system are filtered before a detailed verification with shape verification is run like in the previous years. This is done by a four-direction scan originating from every ball spot that removes objects of wrong size and impossible shape for a ball.

The main challenge introduced by the new ball however lies in its partial similarity with the other objects on the field such as robot feet and goal post. Without depth information, to distinguish between those objects and to still detect a ball lying in front of them, an additional feature-check was added to the ball detection. With this feature-check we are searching for the dark areas on the ball and verify them by size and distribution. The feature size is verified by using the detected ball size as a comparison while the distribution is verified through number and minimum distance between the features. Since all of this can still apply to parts of the robot, especially when dealing with blurry images, a color distribution check was introduced. This simple check discards the possible ball if one part of the scanned region has too much white or black in it. To keep the system calibration free and cope with balls in very bright or shadowy areas, these colors are determined online while verifying the shape of the ball.

Another problem in the detection of a mainly white ball is the possible overlap in the image with other white objects on the field such as lines or robots. To cope with this difficulty we memorize the overlapping areas when using star-like shape verification scan lines from the center of the ball. Size and position of these areas determine if the scanned object lies on a line, in front of another robot or can not be a ball. The feature scan is performed only on a ball with an overlap either with another object (see Fig. 2) or the image border to further reduce the runtime.

III. MOTION

In this section, we will discuss our algorithm utilized since 2007 for biped walking of the Nao. It is already published in parts [3], [4], [5]. The focus of this paper is the presentation



Fig. 2: Detected features on a ball overlapping with the penalty cross.



Fig. 3: Detected ball against the light.

of several details relevant for various aspects of a physical robot, e.g. gravity compensation of undesired elasticities etc. for walking on flat carpets and artificial lawn.

A. Controller

Based on the 3D linear inverted pendulum model (3D-LIPM) [6] where the robot is modeled as a single center of mass (CoM), we utilize a preview controller as proposed by Kajita et al. [7] in a modified version.

The 3D-LIPM relates the movement of a single mass along the x-axis c_x to a Zero Moment Point (ZMP) p , where no torques around the lateral and transversal axis is exerted on the robot:

$$p = c_x - \frac{c_z}{g} \ddot{c}_x. \quad (1)$$

For a linear system the height over ground c_z is constant. The gravity is denoted as g . Given this relation, a discrete-time system can be formulated describing the physical behavior:

$$\mathbf{x}_{k+1} = \mathbf{A}_0 \mathbf{x}_k + \mathbf{b} u_k, \quad (2)$$

where \mathbf{x}_k is the current state of the system, consisting of the CoM position, CoM speed and the ZMP. \mathbf{A}_0 denotes the matrix for predicting the state in the next time frame and \mathbf{b} a vector incorporating the preview controller output u_k into the

system. Details about the controller definition can be found in [3].

B. Gravity and Inertia Compensation

Our sensor feedback methods are able to react to disturbances caused by issues of the physical robot. However, some can be foreseen and should therefore be handled before they occur.

In [8], we show that the robot has unintended flexibilities and elasticities in the gears, links etc. Hence, we proposed [9] the Flexible Linear Inverted Pendulum Model that extends the known 3D-LIPM about a spring-damper-mass system. In the following paragraphs, we describe the gravity and inertia compensation in more detail:

1) General Considerations: As explained in III-A, we utilized the traditional 3D-LIPM on RoboCup 2016 and extended the algorithm by various methods to cope with gravity and inertia issues related to the elasticities.

There are parameters of our walking engine that can be adjusted to lower the impact of flexibilities: The step duration has an effect on the swinging amplitude of the body in y direction (and therefore the lateral acceleration in each step). Thus, it should be chosen to reduce that oscillation by preferring higher step frequencies. Moreover, a larger step height can have a positive impact as the touch-down of the foot on the ground can induce a force/torque supporting the lateral oscillation.

The lateral oscillation is desired for a walk in contrast to an oscillation into the x direction with a growing amplitude. The sensor feedback methods presented in Sec. III-C are intended to reduce these undesired oscillations. Additionally, the configurable hardness of the joints has a huge impact as lower hardness dampens these oscillations. Furthermore, for the swinging foot we lift up the tiptoe that depends on the current height over ground to avoid undesired collisions with the ground.

2) Offsets: Besides these considerations, the algorithm contains possibilities for manual enhancements. For both x and y axis translation and rotational offsets are applicable:

- Translational offset for x and y axis.
 - Fixed, i.e. constant over time.
 - Dynamic, i.e. depending on current speed.
- Rotational offsets.
 - Rotation of body around y axis.
 - * Fixed, i.e. constant over time.
 - * Dynamic, i.e. depending on current speed.
 - Angle offset added to desired joint angles.
 - * Fixed, i.e. always applied.
 - * Dynamic, i.e. applied only if corresponding foot is currently the supporting foot.

Given the foot position in robot coordinate system, a translational offset is added to this position. Thus, it can be avoided to fall more frequently to the back or front.

A rotational offset of the body is applied to ensure a minimum torque on the gears to reduce changing torques that can cause oscillation. The intention of the rotational

offset at the joints is gravity compensation in combination with the undesired elasticities.

C. Sensor Feedback

The motivation to modify the walk by utilizing sensor feedback is evident as not every event can be foreseen. In our approach we combine three different methods, each specialized for a specific domain, that all together utilize every available sensor sources. While we also proposed a method for stabilizing strong pushes [10] the main intention here is to balance smaller disturbances like oscillations, slightly uneven grounds and issues of the physical robot.

1) Observer: An observer can be utilized if the state \mathbf{x}_k cannot be completely measured. In our case we can measure (denoted by \mathbf{y}_y) the position of the CoM by using a forward kinematic and the ZMP utilizing the Foot Resistive Sensors (FSR). The observer equation is comparable to Eq. 2:

$$\hat{\mathbf{x}}(k+1) = \mathbf{A}_0 \hat{\mathbf{x}}_k + \mathbf{L} [\mathbf{y}_y - \mathbf{C}_m \hat{\mathbf{x}}_k] + \mathbf{b} \hat{u}_k. \quad (3)$$

The hat denotes that the corresponding value is now based on the estimation of the observer. Matrix \mathbf{C}_m selects the measurable part of the state:

$$\mathbf{C}_m = \begin{bmatrix} 1 & 0 & 0 \\ 0 & 0 & 1 \end{bmatrix} \quad (4)$$

Details of the method can be found in [5].

2) Orientation Controller: While the observer is based on the linear CoM movement within a plane, a physical robot will tilt and thus leaving this restriction. As rotations are not covered by the above described system, a further control loop is implemented based on the gyroscope measurement $\dot{\varphi}_k$. First, the measured value is filtered (using temporary values $\dot{\varphi}'_k$ and $\dot{\varphi}''_k$):

$$\dot{\varphi}'_k = (1 - \alpha_o) \dot{\varphi}'_{k-1} + \alpha_o \dot{\varphi}_k, \quad (5)$$

$$\dot{\varphi}''_k = (1 - \beta_o) \dot{\varphi}''_k + \beta_o (\dot{\varphi}_k - \dot{\varphi}'_k), \quad (6)$$

with a filter gain α_o and β_o . Next, the desired orientation φ_k^d of the body is calculated by:

$$\varphi_k^d = k_d \dot{\varphi}''_k. \quad (7)$$

Thus, it could be seen as a PD controller based on the filtered orientation with gains $k_p = 0$ and an arbitrary k_d . We apply it for the x axis only.

3) Linear Acceleration: For the observer and orientation controller the acceleration sensor is not utilized. We therefore introduce an additional sensor controller to have all available sensor sources incorporated.

As explained in Sec. III-B, we add a fixed offset to the desired CoM trajectory determined by the controller to optimize the body x position relative to the feet. This controller modifies this value dynamically based on the measured acceleration:

$$x_k^{f,d} = x_k^f - \alpha_a |a_t| \underbrace{\text{sgn}(\bar{a}) \min(|\bar{a}|, 0.03)}_{\in [-0.03, \dots, 0.03]}, \quad (8)$$

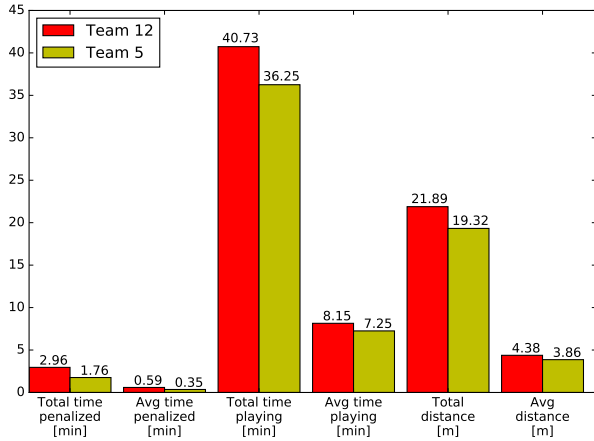


Fig. 4: General statistics of team B-Human (official team number 5) and Nao Devils (official team number 12) for the first half.

where α_a is an arbitrarily chosen gain, $x_k^{f,d}$ the offset added to the feet positions (in robot coordinate system), $sgn()$ the sign function, $min()$ the minimum of the given arguments, a_t the measured acceleration at time t and \bar{a} the mean value of the last five measured accelerations. Basically, Eq. 8 subtracts from the fixed offset the median that is limited to $[-0.03, \dots, 0.03]$ and multiplied with a gain.

D. Acceleration

The controller (Sec. III-A) minimizes but not limits the difference between the desired and actual ZMP. Thus, for high accelerations the actual ZMP may leave the support polygon. We therefore limit the allowed acceleration to a maximum speed change a_{max} within a defined time T : given a speed s_t at time t , the speed at s_{t+T} must fulfill $s_{t+T} - min(s_t, \dots, s_{t+T-1}) < a_{max}$. This also means that deceleration is unlimited.

IV. EVALUATION

To evaluate the performance of an overall system for playing robot soccer outdoor and on artificial grass we decided to analyze the final of the "RoboCup Standard Platform League - Outdoor Competition". It's the idea of the RoboCup not to analyze a specific topic in an isolated situation but to evaluate the combination of the overall system in a practical setup. Team Nao Devils utilized the methods proposed in this paper while the opponent, team B-Human, applied algorithms described in their Team Report 2016. Fig. 4 and Fig. 5 depicts general statistics for the first half of the final and the second half respectively.

A. Motion

Evaluations of motion algorithms concentrate generally on specific setups in isolated situations with only a few iterations. A robot soccer game on artificial grass has the advantage to evaluate the system outside a laboratory. Several criteria decide about a successful walk and game. Besides usual criteria as the avoidance of falling while achieving

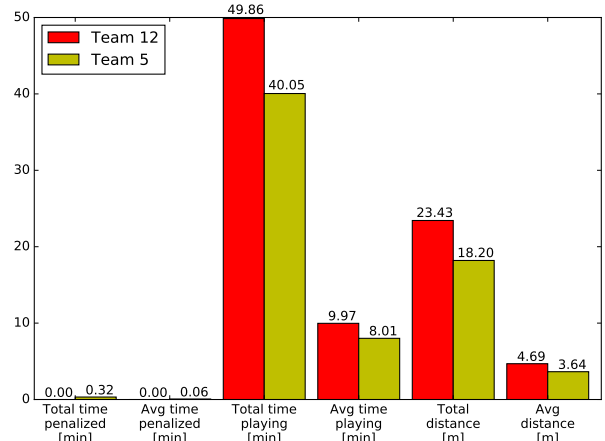


Fig. 5: General statistics of team B-Human (official team number 5) and Nao Devils (official team number 12) for the second half.

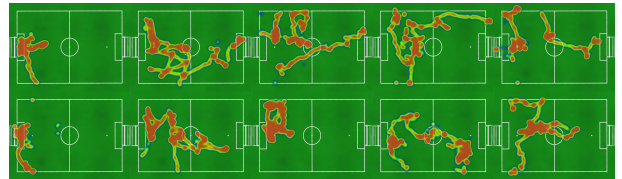


Fig. 6: Heatmap of team B-Human for (from left to right) robots 1 to 5 and for 1st half time (upper row) and 2nd half (lower row).

high speeds, the exact execution of the desired speed, stable camera images and low power consumption to avoid overheating of the motors are also significant. It must be noted that the drawback of this kind of evaluation is the missing possibility of recording ground truth data.

For both team there is a small trend to more frequent fall-downs as the game advances. This can be the result of the temperature of the motors leading to an intentional limitation of the torque to avoid overheating.

Fig. 8 depicts for every minute of the game how often Team B-Human and Nao Devils fell down. This count contains exclusively fall-downs during walking, i.e. the robot did not touch any obstacles. The total number of fall-downs is 82 and 40 of team B-Human and Nao Devils respectively. As this number is influenced by the total distance traveled by all



Fig. 7: Heatmap of team Nao Devils for (from left to right) robots 1 to 5 and for 1st half time (upper row) and 2nd half (lower row).

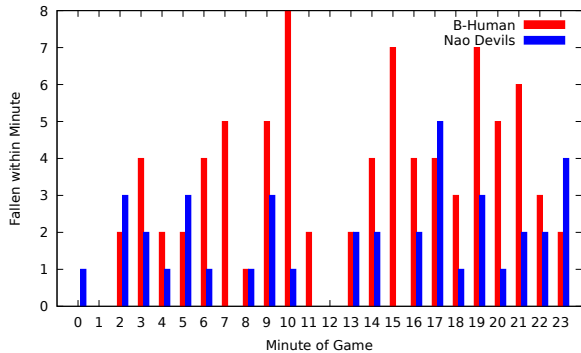


Fig. 8: Total number of fall-downs for each team and minute of the game. In minute 12 the first half-time ended and the second begun, thus there are no fall-downs.

robots during game play and game ready state¹, we introduce a metric "fall-downs per meter". It is $2.19 \frac{\text{Fall-Down}}{\text{m}}$ for B-Human and $0.88 \frac{\text{Fall-Down}}{\text{m}}$ for Nao Devils. Please note that the distance is measured utilizing the self-localization of the robots where we removed impossible large jumps from one frame to the next ($> \frac{40\text{mm}}{200\text{ms}}$). Therefore, this is an approximation that relies on the quality of the localization system.

Fig. 6 and Fig. 7 depict the heat maps for all robots of team B-Human and Nao Devils respectively. It can be seen that Nao Devils try to stay locally at a predefined point to avoid traveling long distances. However, as Fig. 4 and Fig. 5 indicates the traveled distances per robot are comparable.

B. Vision

During the outdoor match a cloudy sky changed several times with a bright sunny day which presented a good test for the adaptivity of our vision system. As in the previous RoboCups, no calibration of the vision system had to be done in the outdoor or indoor environment. Our approach allowed us to play with auto camera settings (auto exposure and auto white balance) indoor as well as outdoor at RoboCup 2016.

In the entire match our team was able to maintain a stable localization and keep the ball in sight. Both teams did not lose sight of the ball for more than 20 seconds, although the ball detection of Team B-Human proved to be more reliable, especially in larger distances.

In the instances where we lost sight of the ball, the ball was lying either next to another robot or in a shadow surrounded by sunlight. This indicates, that our feature scan for the ball as well as our dynamic color detection for field color (see [1]) is not sufficient in this difficult scenario.

V. CONCLUSION

This paper summarized our methodologies to play robot soccer in an outdoor-like environment. In particular, the paper showed that the walking engine developed within the last decade, is robust against different floor types without

¹In the game ready phase the robots walk to their initial positions before game start

making major conceptual changes. Hence, special focus for artificial grass lies on stabilizing sensor control of the upper body movement of the robot. This way, our walking engine provides even without reactive stepping, i.e. additional steps to balance out disturbances, promising results.

It is certainly true that ball detection is an essential problem in outdoor soccer play. This is due to the difficult setup that does no longer contain any kind of color information as well as shadows and continuous changes in lighting. While there was no need to change the heuristic approach of our vision system, we made a number of minor adaptations and improvements to achieve reasonable detection rates.

REFERENCES

- [1] I. Schwarz, M. Hofmann, O. Urbann, and S. Tasse, "A robust and calibration-free vision system for humanoid soccer robots," in *Robot Soccer World Cup*. Springer, 2015, pp. 239–250.
- [2] R. T. Committee, "Robocup standard platform league (nao) rule book," 2016.
- [3] S. Czarnetzki, S. Kerner, and O. Urbann, "Observer-based dynamic walking control for biped robots," *Robotics and Autonomous Systems*, vol. 57, no. 8, pp. 839–845, 2009.
- [4] ——, "Applying dynamic walking control for biped robots," in *RoboCup 2009: Robot Soccer World Cup XIII*. Springer Berlin Heidelberg, 2010, pp. 69–80.
- [5] O. Urbann and S. Tasse, "Observer based biped walking control, a sensor fusion approach," *Autonomous Robots*, vol. 35, no. 1, pp. 37–49, 2013.
- [6] S. Kajita, F. Kanehiro, K. Kaneko, K. Fujiwara, K. Yokoi, and H. Hirukawa, "A realtime pattern generator for biped walking," in *ICRA*. IEEE, 2002, pp. 31–37.
- [7] ——, "Biped walking pattern generator allowing auxiliary zmp control," in *IROS*. IEEE, 2006, pp. 2993–2999.
- [8] O. Urbann, S. Kerner, and S. Tasse, "Rigid and Soft Body Simulation Featuring Realistic Walk Behaviour," in *RoboCup 2011: Robot Soccer World Cup XV Preproceedings*. RoboCup Federation, 2011.
- [9] O. Urbann, I. Schwarz, and M. Hofmann, "Flexible linear inverted pendulum model for cost-effective biped robots," in *Humanoid Robots (Humanoids), 2015 15th IEEE-RAS International Conference on*, Nov 2015, pp. 128–131.
- [10] O. Urbann and M. Hofmann, "A reactive stepping algorithm based on preview controller with observer for biped robots," in *Intelligent Robots and Systems (IROS), 2016 IEEE/RSJ International Conference on*, 2016, p. akzeptiert.